Supporting Information

Guardado-Mendoza et al. 10.1073/pnas.0906471106

SI Materials and Methods

Analytical Measurements and Metabolic Parameters. FPG was measured by the glucose oxidase method with the SYNCHRON CX System (Beckman Coulter, Inc), HbA1c by the HPLC method, plasma insulin concentration by RIA (Linco Research), plasma glucagon concentration by RIA (Euro-Diagnostica AB), and FFA FFA concentration with a fluorometric method (WAKO HR Series NEFA-HR). Insulin resistance was estimated by using the homeostasis model assessment and insulin secretion by using the HOMA-β cell function, as previously described (1). The adipose tissue insulin resistance index was also calculated as the result of FFA $\times$ FPI.

Molecular Cloning and Sequencing of Baboon IAPP. Total RNA was isolated from the pancreas of 3 baboons using TRIzol Reagent (Molecular Research Center). RNA was treated with RQ1 DNase (Promega) for 30 min to eliminate traces of DNA. Two micrograms of total RNA were used in a reverse transcription (RT) reaction using the MLV reverse transcriptase by Ambion and 200 ng per reaction of random primers by Invitrogen, according to manufacturer's directions. IAPP was amplified by PCR under the following conditions: 94 °C for 5 min followed by 40 cycles of 94 °C $\times$ 45", 55 °C $\times$ 45", and elongation step of 72 °C $\times$ 45". A final elongation step of 72 °C for 10 min was conducted. The PCR products were analyzed in a 2% agarose gel stained with ethidium bromide. PCR reactions were digested with a mixture of exonuclease I and shrimp phosphatase (1:2) for 30 min at 37 °C followed by denaturation at 80 °C. The sequencing reaction was conducted with Big dye terminator (Applied Biosystems) according to manufacturer's directions. Primers used for cloning and sequencing baboon IAPP were as follows: Forward 1 TGCTGTTGGGGGTTTTATTC, Reverse 1 CCTGAGCCCAGAAAGTCAAG, Forward 2 GCTTGGACTCTTTTCTTGAAGC, Reverse 2 CGTTCTTAAACCTGTGCCACT.

The primers were designed on Primers 3.0 using the predicted sequence for rhesus monkey IAPP (XM 001098290). Sequences were analyzed in a 3100 DNA analyzer (Applied Biosystems). The obtained data were aligned using the Sequencer v 4.0 software and compared with the human sequence in BLAST (www.ncbi.nlm.nih.gov/blast) and compared with amylin sequences of other species using ClustalW (www.Clustalw.org).

Fibrillogenic Propensities of Baboon IAPP. Fibrillogenic propensities of baboon and human IAPP were predicted using a structure-based algorithm originally described by Thompson et al. (2). This algorithm uses the crystal structure of the fibril-forming peptide NNQQNY from the sup35 prion protein of *Saccharomyces cerevisiae*, which makes up the cross-beta spine of amyloid-like fibrils (3). Each 6-residue peptide not containing a proline from the full-length sequence of IAPP is threaded onto the NNQQNY structure backbone, and the energetic fit is evaluated using the Rosetta Design program. Additionally, the quality of the steric-zipper interface is compared in terms of shape complementarity and surface area to other amyloid-like peptides reported by Sawaya et al. (4). Based on these experimental amyloid-like peptide structures, an energy threshold of -23 kcal/mol was chosen. Segments with energies equal to or below this threshold are deemed to have high fibrillogenic propensity. The energies of all hexameric peptides were plotted with the indicated residue being the first residue of the hexameric segment. Each segment is color-coded according to its energy, which is representative of fibrillogenic propensity.

Electron Microscopy. A subgroup of pancreases with IA underwent electron microscopy immunocytochemistry. Samples were fixed for 2 h at 4 °C in a mixture of 2% paraformaldehyde and 0.5% glutaraldehyde in 0.05 M pH 7.3 cacodylate buffer, and embedded in London White Resin. Thin sections, after incubation with ovalbumin 1% in TBS 0.05M pH 7.4 for 5 min at room temperature, were incubated for 24 h at 4 °C with anti-IAPP antibody (Peninsula Laboratories Inc.), then with 1:50 gold-tagged goat anti-rabbit (EY Laboratories) for 1 hour at room temperature, and finally counterstained with uranyl acetate and lead citrate. Specificity controls consist of omission of the first layer and use of tissues with or without pertinent antigens. Thin sections are examined with a Philips (Morgagni 268 D) electron microscope.

Morphometric Analysis. Morphometric analysis was performed using the Computer Assisted Stereology Toolbox (CAST) 2.0 system from Olympus and using the stereology fundaments previously described on pancreatic sections randomly collected from the pancreas body and tail (5, 6). The operator was blinded to the metabolic status of the baboon and the reproducibility of the measurements was estimated twice in 5 specimens with a coefficient of variation less than 5%. Each field was selected randomly using the CAST meander sampling. We analyzed 84 $\pm$ 39 mm^2 of pancreatic tissue and 106 $\pm$ 48 islets per animal. In each field, point counting of total pancreatic tissue, islets, and amyloid deposits was performed at the magnification of 40$\times$ to calculate the relative volume of each component. Relative islet and amyloid volumes were calculated by using the following formulas: (*i*) relative islet volume: (IP/TP) $\times$ 100, where IP = points that hit islet cells and TP = total pancreas points; (*ii*) relative amyloid volume: (IA/TP) $\times$ 100, where IA = points that hit amyloid deposits. Total pancreatic points averaged 9,598 $\pm$ 3,203 per slice per baboon. Stereology was also applied to calculate the relative amyloid area (percentage of islet area occupied by amyloid deposits) by using the formula (2 $\times$ I/LT), where I = number of intersections made by the lines with respect to the structure under study for all fields per slice (4,799 $\pm$ 1,601 lines evaluated per slice/baboon) and LT = total line length. Relative amyloid area was calculated by superimposing a series of test lines (line length = 54.4 μm) in a random orientation on the histological images and counting the intersections with the structure of interest. These 2 measurements of IA severity (relative amyloid volume and relative amyloid area) were tightly correlated ($r = 0.977$, $P < 0.0001$). An additional analyzed parameter were the islet density being the number of islets per screened tissue area expressed in mm^2, mean-islet size (total area occupied by the islets in μm^2 divided by the total number of islets in that specific area) and amyloid prevalence (percentage of islets with any degree of amyloid deposition). The quantification of the relative β-cell volume/islet was done by dividing the total points that hit β cells over the total number of points that hit pancreatic islets. The same method was used for quantification of the relative α-cell volume. The relative β- and α-cell volume was measured in 40 baboons randomly selected and with different levels of IA and FPG. Measurement of α-cell numbers and size was done in the 20 cases used for the Ki67 and M30 staining. Counting of the α cells was performed in the glucagon stains, and at least 30 islets were randomly selected per case and analyzed

using the CAST meander sampling; α-cell size (μm^2) was estimated inserting a unique point inside the cell and several probe lines and marking the intersections between the border cell and the probe lines.

Immunofluorescence Staining. Sections 3-μm thick were fixed and immunostained as previously described (7). Briefly, after antigen retrieval by microwave heating in citrate buffer, sections were immunostained with the anti-Ki67 antibody (4 °C for 18–20 h), followed by incubation with biotin-conjugated anti-rabbit and FITC-conjugated streptavidin. To visualize α and β cells, sections were then stained with anti-glucagon and anti-insulin antibodies (2 h at room temperature) followed by TRITC- and CY5-conjugated secondary reagents. The following antibodies were used: anti-insulin guinea pig monoclonal (Linco), anti-glucagon rabbit polyclonal (Milab), and anti-Ki67 mouse monoclonal (clone MIB1, Dako). Secondary antibodies were from Jackson ImmunoResearch. Islets were imaged using a Bio-Rad MRC 1024 confocal laser scanning microscope. To reduce the bleed through, confocal images were acquired sequentially, using the LaserSharp2000 software with a low iris diameter (1–2). The fluorophores (FITC, TRITC, and Cy5) are all commonly used for triple immunostaining and the bleed-through for these fluorophores is negligible when sequential scanning is used. Background signal caused by nonspecific binding was subtracted from "test" images.

1. Matthews DR, et al. (1985) Homeostasis model assessment: insulin resistance and beta-cell function from fasting plasma glucose and insulin concentrations in man. *Diabetologia* 28:412–419.
2. Thompson MJ, et al. (2006) The 3D profile method for identifying fibril-forming segments of proteins. *Proc Natl Acad Sci USA* 103:4074–4078.
3. Nelson R, et al. (2005) Structure of the cross-beta spine of amyloid-like fibrils. *Nature* 435:773–778.
4. Sawaya MR, et al. (2007) Atomic structures of amyloid cross-beta spines reveal varied steric zippers. *Nature* 447:453–457.
5. Freere RH, Weibel ER (1967) Stereologic techniques in microscopy. *J Royal Microsc Soc* 87:25–34.
6. Mandarim-de-Lacerda CA (2003) Stereological tools in biomedical research. *An Acad Bras Cienc* 75:469–486.
7. Federici M, et al. (2001) High glucose causes apoptosis in cultured human pancreatic islets of Langerhans: a potential role for regulation of specific Bcl family genes toward an apoptotic cell death program. *Diabetes* 50:1290–1301.

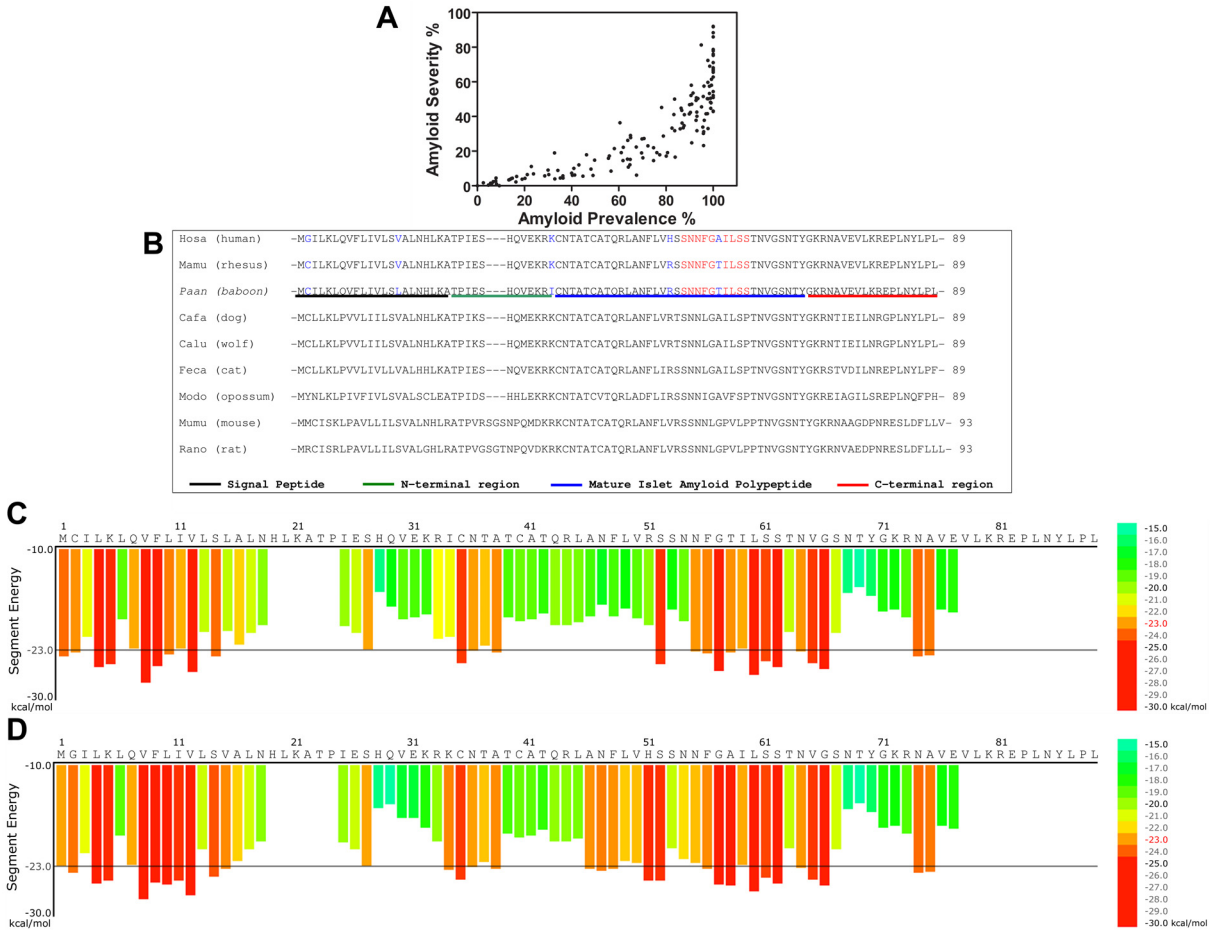

Fig. S1. Amyloid severity and prevalence in baboons and sequence-fibrillogenic propensities of the baboon IAPP. Relation between amyloid severity and amyloid prevalence (*A*), amino acid sequence of the baboon amylin peptide compared with other species (*B*). Fibrillogenic propensities of the baboon (*C*) and human IAPP (*D*) predicted with the 3-D profile method using the NNQQNY backbone. Segments with Rosetta energies of −23 kcal/mol or lower (orange-red) are predicted to have high fibrillogenic propensity.

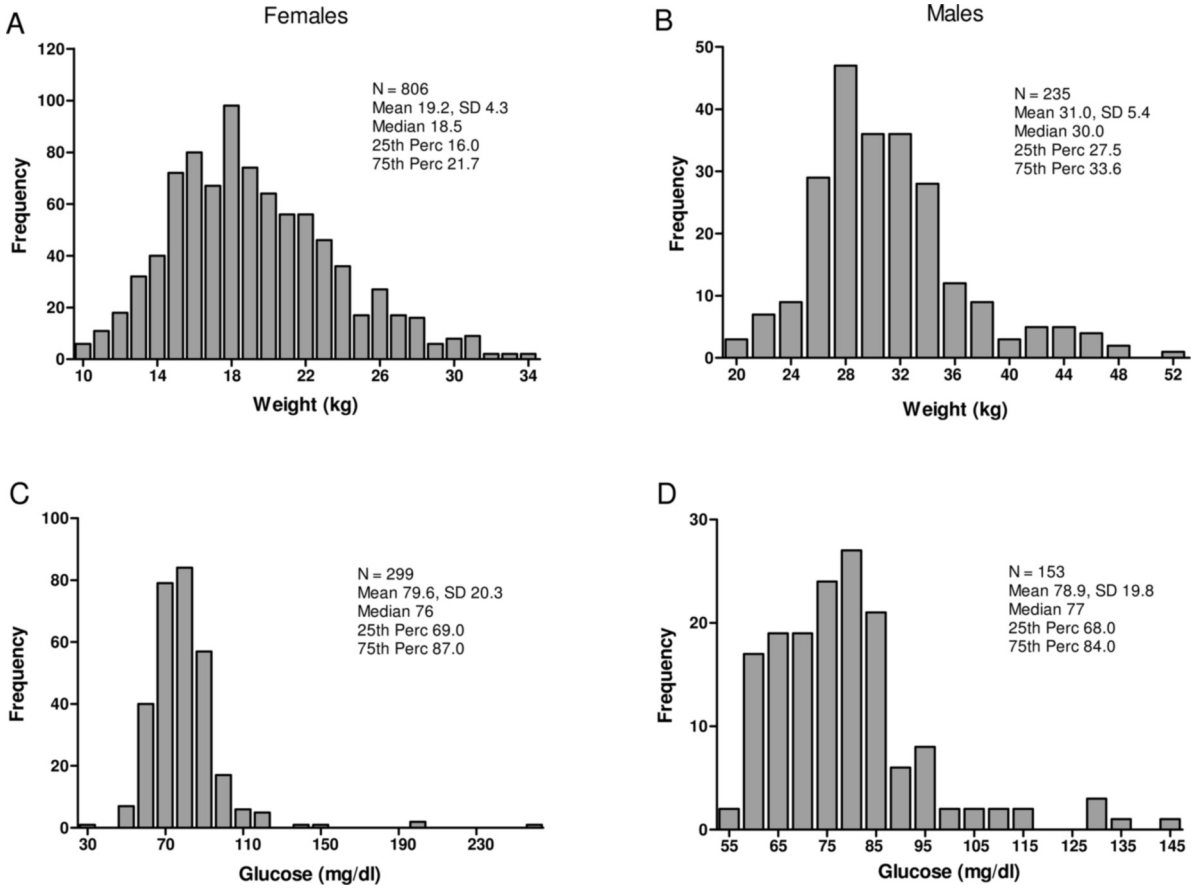

Fig. S2. Distribution of body weight (kg) and glucose concentration (mg/dL) in adult female (*A* and *C*) and male (*B* and *D*) baboons.

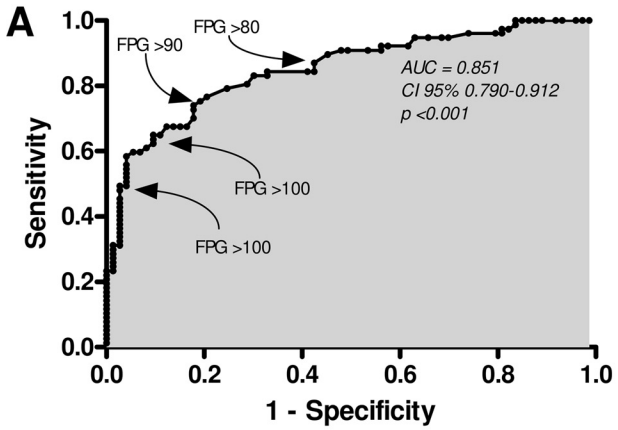

B

Glucose (mg/dl)	Prev (%)	Se (%)	Sp (%)	PPV (%)	NPV (%)	LR
>80	68	87	58	67	83	2.07
>90	81	74	83	80	75	4.35
>100	92	59	95	92	69	11.80
>110	95	45	98	94	62	22.50

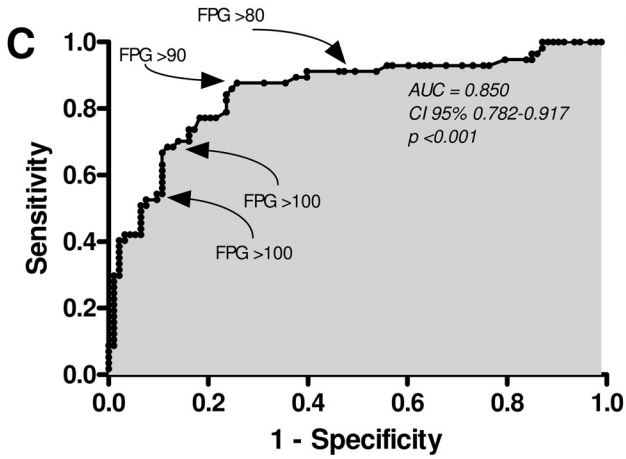

D

Glucose (mg/dl)	Prev (%)	Se (%)	Sp (%)	PPV (%)	NPV (%)	LR
>80	51	91	51	51	90	1.86
>90	68	84	77	68	90	3.65
>100	78	68	89	78	82	6.18
>110	81	52	93	81	76	7.43

Fig. S3. ROC curve, Prevalence (Prev = % of baboons with amyloid severity >25 and >40%), Sensitivity (Se), specificity (Sp), positive predictive value (PPV), negative predictive value (NPV), and likelihood ratio (LR) for different fasting plasma glucose concentrations to predict amyloid deposits in >25% (*A* and *B*) and in >40% (*C* and *D*) of islet area.

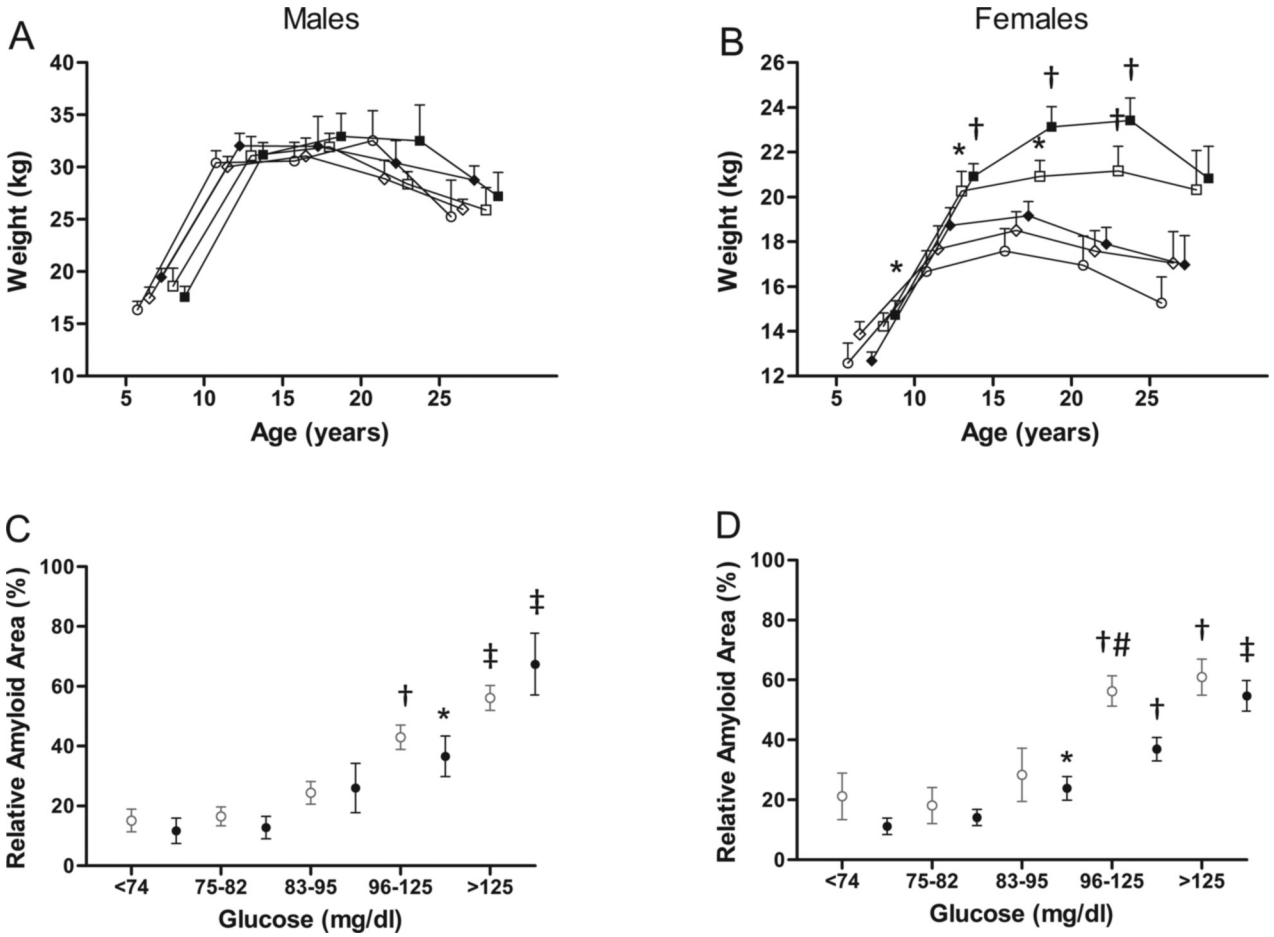

Fig. S4. Weight at 5, 10, 15, 20, and 25 years of age in male (*A*) and female (*B*) baboons according to the severity of amyloid deposition at death (open circles Group 1, open diamonds Group 2, filled diamonds Group 3, open squares Group 4, and filled squares Group 5). (*C*) Relationship between relative amyloid area and FPG levels in females (open circles) and males (filled circles). ∗, $P < 0.05$ for comparison vs. Group 1 and 2; †, $P < 0.05$ for comparison vs. Groups 1, 2, and 3; ‡, $P < 0.05$ for comparison vs. all groups. (*D*) Relative amyloid area according to FPG concentration in overweight (open circles) and nonoverweight (filled circles) baboons. #, $P < 0.05$ for comparison vs. nonoverweight group within the same glucose levels.

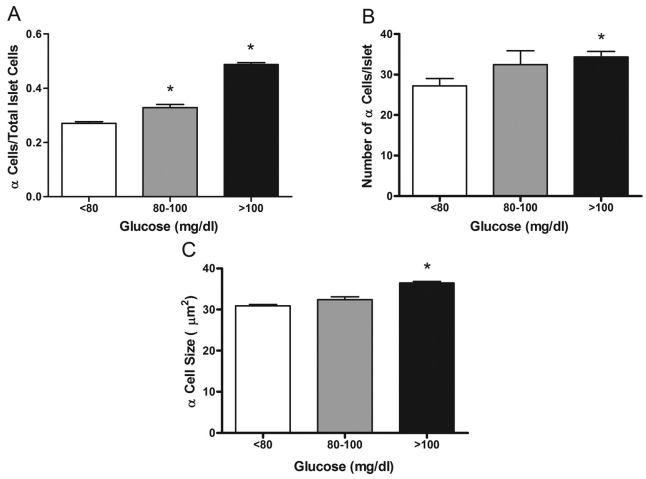

Fig. S5. Number of α cells/total islet cells (*A*); number of α cells/islet (*B*), and α cell size according to FPG (*C*). *, $P < 0.05$ vs. control group.

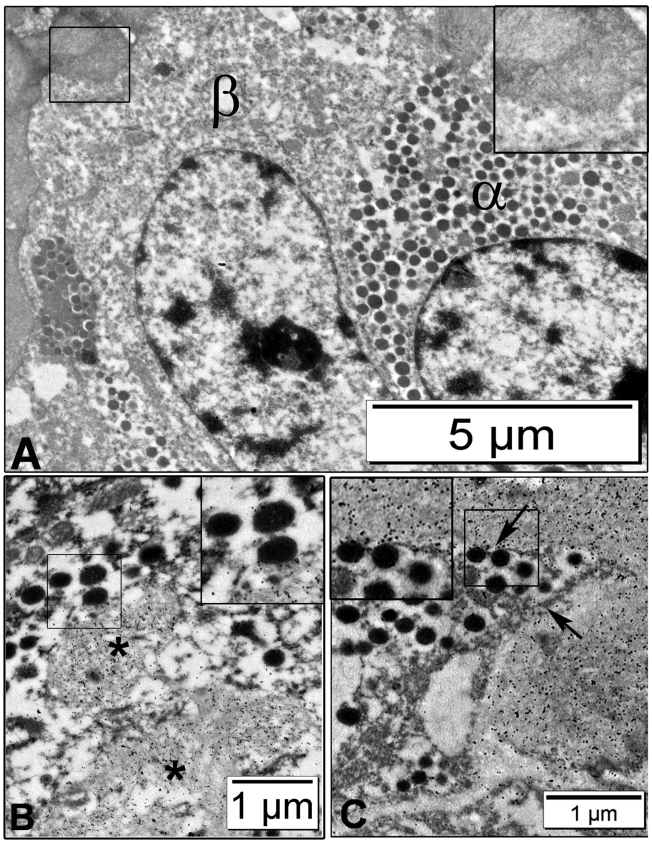

Fig. S6. Electron microscopy examination reveals abundant fibrillar deposits in the cytoplasm of a sparsely granulated β cell (β) and in the extracellular space, where they are more compact (*Inset*); in the same picture an α cell (α) with numerous secretory granules and lacking cytoplasmic fibrillar deposits is evident (*A*). In the β cell, the intracytoplasmic deposits (asterisk) show irregular borders without a membrane, are close and attached to secretory granules and are strongly positive for IAPP, as demonstrated by immunogold staining (*B*). (*C*) A detail of extracellular amyloid deposits that are strongly IAPP-positive and are clearly separated from the cytoplasm of a well-granulated endocrine cell (*Left*) by an evident cell membrane (arrows). Details are shown in the insets.

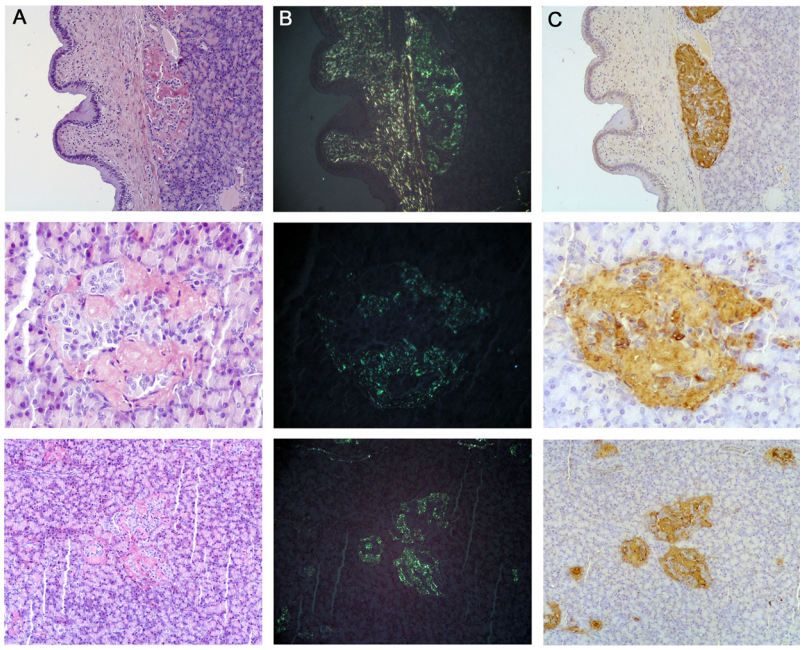

Fig. S7. Congo red stains and IAPP immunohistochemistry performed in consecutive sections of 3 different cases of diabetic baboon pancreases. Amorphous globules of amyloid that replace islet cells are stained in red using Congo red stain (*A*) and show the typical green birefringence in polarized light (*B*). Islet amyloid is composed of IAPP as demonstrated by immunohistochemical staining with anti-IAPP antibody (*C*).

Table S1. Morphometric analysis of the pancreases of 150 baboons divided according to the severity of islet amyloid deposition (relative amyloid area)

Variable	Group 1 IA < 5.5% ($n = 30$)	Group 2 IA 5.5–17% ($n = 30$)	Group 3 IA 18–35% ($n = 30$)	Group 4 IA 36–51% ($n = 30$)	Group 5 IA > 51% ($n = 30$)	*P* group
Mean islet size, μm^2	8,227 ± 468	9,471 ± 742	9,255 ± 465	11,091 ± 725[a]	12,819 ± 947[a,b,c]	<0.001
Relative islet volume, % of total pancreas	2.6 ± 0.2	3.4 ± 0.3	3.4 ± 0.2	4.1 ± 0.4[a]	5.4 ± 0.7[a,b,c,d]	0.001
Islet density, islets/mm^2	3.1 ± 0.2	3.6 ± 0.3	3.8 ± 0.2	3.6 ± 0.2	4.0 ± 0.3[a]	0.013
Relative amyloid volume, % of total pancreas	0.5 ± 0.1	0.5 ± 0.1	1.1 0.2[a,b]	1.8 ± 0.4[a,b,c]	2.4 ± 0.4[a,b,c,d]	<0.001
Relative amyloid area, % of islet	2.2 ± 0.3	11.0 ± 0.8[a]	26.7 ± 1.0[a,b]	44.8 ± 0.8[a,b,c]	67.5 ± 2.2[a,b,c,d]	<0.001

[a]$P < 0.05$ for comparisons vs. Group 1.
[b]$P < 0.05$ for comparisons vs. Group 2.
[c]$P < 0.05$ for comparisons vs. Group 3.
[d]$P < 0.05$ for comparisons vs. Group 4.

Table S2. Body weight during life and fasting plasma glucose during the last 4 years of life in baboons stratified according to severity of amyloid deposition

Variable	Group 1 amyloid < 5.5% (n = 30) <5.5%	Group 2 amyloid 5.5–17% (n = 30)	Group 3 amyloid 18–35% (n = 30)	Group 4 amyloid 36–51% (n = 30)	Group 5 amyloid > 51% (n = 30)	P group
Sex, F/M	14/16	18/12	25/5	20/10	24/6	0.007
Age, years	16.2 ± 0.9	19.3 ± 0.8[a]	19.8 ± 0.9[a]	19.9 ± 0.9[a]	21.6 ± 0.6[a]	0.001
Weight, kg						
No. of females	14	18	25	20	24	
5 years of age	12.5 ± 0.9	13.8 ± 0.5	12.6 ± 0.4	14.2 ± 0.6	14.7 ± 0.6[a,c]	0.011
10 years of age	16.6 ± 0.9	17.6 ± 1.0	18.7 ± 0.8	20.2 ± 0.8[a,b]	20.9 ± 0.5[a,b,c]	0.004
15 years of age	17.6 ± 1.0	18.5 ± 0.8	19.1 ± 0.6	20.9 ± 0.7[a,b]	23.1 ± 0.9[a,b,c]	0.001
20 years of age	16.9 ± 1.3	17.5 ± 0.9	17.9 ± 0.7	21.2 ± 1.1[a,b,c]	23.4 ± 1.0[a,b,c]	0.001
Last weight	15.7 ± 0.6	16.2 ± 0.8	15.8 ± 0.7	18.9 ± 1.2[c]	21.4 ± 1.3[a,b,c]	0.001
Maximum weight	19.8 ± 1.0	20.0 ± 0.9	20.3 ± 0.8	23.6 ± 0.9[a,b,c]	25.7 ± 0.8[a,b,c]	0.001
Overweight at age 10 (%)	1 (7.1%)	3 (16.6%)	4 (16.0%)	7 (35.0%)	10 (41.6%) [a]	0.03
Overweight at age 15 (%)	2 (14.2%)	3 (16.6%)	6 (24.0%)	9 (45.0%)	12 (50.0%)[a,b]	0.02
Overweight at age 20 (%)	1 (7.1%)	1 (5.5%)	2 (8.0%)	10 (50.0%)[a,b,c]	15 (62.5%)[a,b,c]	0.002
Overweight at death (%)	1 (7.1%)	1 (5.5%)	2 (8.0%)	6 (30.0%)	9 (37.5%)[a,b,c]	0.042
Weight, kg						
No. of males	16	12	5	10	6	
5 years of age	16.3 ± 0.8	17.4 ± 1.0	19.4 ± 0.8	18.6 ± 1.7	17.5 ± 1.0	0.452
10 years of age	30.4 ± 1.1	30.0 ± 0.9	32.0 ± 1.2	31.0 ± 1.8	31.2 ± 1.1	0.911
15 years of age	30.6 ± 1.8	31.0 ± 1.7	32.0 ± 2.9	31.9 ± 1.3	32.9 ± 2.2	0.926
20 years of age	32.5 ± 2.9	28.9 ± 1.7	30.4 ± 2.1	28.3 ± 1.2	32.5 ± 3.4	0.668
Last weight	30.2 ± 2.0	29.2 ± 1.5	29.6 ± 1.4	29.8 ± 2.1	30.7 ± 3.6	0.993
Maximum weight	33.2 ± 1.9	33.5 ± 1.6	33.2 ± 1.8	33.8 ± 1.7	35.4 ± 2.6	0.968
Overweight at age 10 (%)	2 (12.5%)	2 (16.6%)	1 (25.0%)	2 (25.0%)	1 (16.6%)	0.67
Overweight at age 15, (%)	2 (12.5%)	2 (16.6%)	1 (25.0%)	1 (10.0%)	2 (33.3%)	0.488
Overweight at age 20, (%)	2 (12.5%)	2 (16.6%)	1 (25.0%)	0	2 (33.3%)	0.941
Overweight at death, (%)	2 (12.5%)	3 (25.0%)	1 (25.0%)	2 (25.0%)	1 (16.6%)	0.79
FPG, mg/dL						
At death	75 ± 2	83 ± 3	96 ± 7	115 ± 7[a,b]	187 ± 21[a,b,c,d]	0.001
1 year before	87 ± 6	86 ± 7	77 ± 4	84 ± 4	168 ± 29[a,b,c,d]	0.001
2 years before	83 ± 5	79 ± 3	70 ± 4	89 ± 6	113 ± 33[a,b,c]	0.047
3 years before	81 ± 5	84 ± 2	85 ± 11	86 ± 6	84 ± 10	0.989

FPG, fasting plasma glucose.
[a]$P < 0.05$ for comparisons vs. Group 1.
[b]$P < 0.05$ for comparisons vs. Group 2.
[c]$P < 0.05$ for comparisons vs. Group 3.
[d]$P < 0.05$ for comparisons vs. Group 4.

Table S3. Univariate and multivariate regression analyses for the prediction of amyloid severity (relative amyloid area, %)

	Univariate analysis			Multivariate analysis		
	r	*P* value		Partial *R*	*P* value	*F* value
			Model 1			
Age, years	0.330	<0.001	Age, years	0.325	<0.001	18
Sex (1 = F, 2 = M)	−0.248	0.009	Sex (1 = F, 2 = M)	0.06	0.498	<4
Overweight at 15 years (1 = yes, 2 = no)	−0.268	<0.001	Overweight at 15 years (1 = yes, 2 = no)	−0.17	0.054	<4
FFA, mEq/L	0.269	0.001	FFA (mEq/L)	−0.11	0.203	<4
ln(glucose)	0.691	<0.001	ln(glucose)	0.646	<0.0001	121
ln(glucagon)	0.254	0.003	ln(insulin)	−0.05	0.609	<4
ln(insulin)	−0.090	0.290	ln(glucagon)	0.002	0.978	<4
			Adjusted R^2	0.535	<0.0001	
			Model 2			
			Age, years	0.310	<0.001	
			ln(glucose)	0.680	<0.001	
			Adjusted R^2	0.519	<0.001	